

QUT Digital Repository:
<http://eprints.qut.edu.au/>



Frost, Ray L. (2009) *Tlapallite* $H_6(Ca,Pb)_2(Cu,Zn)_3SO_4(TeO_3)_4TeO_6$, a multi-anion mineral: A Raman spectroscopic study. *Spectrochimica Acta Part A: Molecular and Biomolecular Spectroscopy*, 72(4). pp. 903-906.

© Copyright 2009 Elsevier

1 **Tlapallite $H_6(Ca,Pb)_2(Cu,Zn)_3SO_4(TeO_3)_4TeO_6$ –a multi anion mineral**
2 **-a Raman spectroscopic study**

3
4 **Ray L. Frost** •

5
6 Inorganic Materials Research Program, School of Physical and Chemical Sciences,
7 Queensland University of Technology, GPO Box 2434, Brisbane Queensland 4001,
8 Australia.

9
10
11 **ABSTRACT**

12
13 Tellurates may be subdivided according to formula and structure. There are three
14 types of tellurate minerals: type (a) $(AB)_m(TeO_4)_pZ_q$, type (b) $(AB)_m(TeO_6).xH_2O$ and
15 type (c), compound tellurates in which a second anion is involved. Tlapallite, a multi
16 anion mineral containing both tellurate and tellurite units, as well as sulphate, is an
17 example of type (a). Tellurates are rare minerals as the tellurate ion is easily reduced
18 to the tellurite ion. Raman bands at 691, 708, 764 and 796 cm^{-1} are attributed to
19 $(TeO_6)^{2-}$ and $(TeO_3)^{2-}$ stretching bands. The intense sharp Raman band at 973 cm^{-1} is
20 assigned to the $\nu_1 (SO_4)^{2-}$ symmetric stretching mode, whilst the two bands at 1062
21 and 1104 cm^{-1} are assigned to the $\nu_3 (SO_4)^{2-}$ antisymmetric stretching mode. The
22 spectral region 100 to 600 cm^{-1} displays the bands which are attributable to the $(SO_4)^{2-}$,
23 $(TeO_3)^{2-}$ and $(TeO_6)^{4-}$ bending modes. Some evidence from very low intensity
24 Raman bands in the 2800 to 3600 cm^{-1} region provides evidence of proton-
25 tellurate/tellurite anion interactions.

26
27 **Keywords:** Tellurate, Tellurite, Tlapallite, Raman Spectroscopy, Rodalquilarite

28
29
30
31
32

• Author to whom correspondence should be addressed (r.frost@qut.edu.au)
Tel. +61 7 3138 2407 Fax +61 7 3138

33

34 1. Introduction

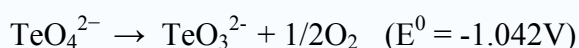
35

36 There exists in nature, a collection of minerals based upon the elements
37 selenium and tellurium. These minerals are the tellurates/selenates and the
38 tellurites/selenites. They minerals may be subdivided into groups according to
39 formula and structure [1]. There are five groups based upon the formulae (a) $A(XO_3)$,
40 (b) $A(XO_3)_x \cdot H_2O$, (c) $A_2(XO_3)_3 \cdot xH_2O$, (d) $A_2(X_2O_5)$ and (e) $A(X_3O_8)$. Of the
41 selenites, molybdomenite is an example of type (a); chalcomenite, clinochalcomenite,
42 cobaltomenite and ahlfeldite are examples of type (b) mandarinoite is an example of
43 type (c). There are no known examples of selenite minerals with formulae (d) and
44 (e). The tellurite group, however, consists of minerals that can be categorised into
45 each of the five formula types. Tellurates are very rare minerals because the tellurate
46 anion is very easily reduced to the tellurite anion. There are three types of tellurate
47 minerals: type (a) $(AB)_m(TeO_4)_p Z_q$, type (b) $(AB)_m(TeO_6)_x \cdot H_2O$ and type (c),
48 compound tellurates in which a second anion is involved. An example of type (a) is
49 the mineral xocomecatlite [2-4]. Kuranakhite is also an example from this group.
50 Xocomecatlite, $Cu_3TeO_4(OH)_4$, is related to the mineral tlalocite,
51 $Cu_{10}Zn_6(TeO_3)(TeO_4)_2Cl(OH)_{25} \cdot 27H_2O$. Both originate from Moctezuma, Sonora,
52 Mexico. Another related tellurate mineral is tlapallite
53 $H_6(Ca,Pb)_2(Cu,Zn)_3SO_4(TeO_3)_4TeO_6$ which is a mixed anionic mineral containing
54 both tellurate and tellurite anions.

55

56 In contrast to the extensive list of tellurites, there are very few tellurate
57 minerals. The tellurate ion can be either TeO_4^{2-} or TeO_6^{6-} . Unlike sulphate, tellurate
58 is a good oxidizing agent; it can be reduced to tellurite or tellurium. The E^0 value is
59 significant as it gives an indication of the strength of the tellurate ion as an oxidising
60 agent.

61



62

63

64

65

Tellurate exists in two forms, metatellurate ion, TeO_4^{2-} , and orthotellurate ion,
 TeO_6^{6-} . Compounds include both metatellurates and orthotellurates. Metatellurates
are analogous to sulfates, however, they are rare. Orthotellurates are much more
common and therefore forms most of the chemistry of tellurates. In neutral

66 conditions, pentahydrogen orthotellurate ion, H_5TeO_6^- , is most common; in basic
67 conditions, tetrahydrogen orthotellurate ion, $\text{H}_4\text{TeO}_6^{2-}$, is most common and in acid
68 conditions, the orthotelluric acid, H_6TeO_6 , is more common. The number of tellurate
69 minerals is greatly overshadowed by the number of tellurites minerals, minerals
70 containing TeO_3^{2-} units. A mineral which contains both tellurate and tellurite anions
71 is the mineral tlapallite. The powder X-ray diffraction patterns obtained by Williams
72 and Duggan showed that the mineral was monoclinic with a formula
73 $\text{H}_6\text{Ca}_2\text{Cu}_3(\text{SO}_4)(\text{TeO}_3)_4\text{TeO}_6$ with a $\text{Te}^{4+}/\text{Te}^{6+}$ ratio 4 [5].

74
75
76 Raman spectroscopy has proven very useful for the study of minerals [6-10].
77 Indeed, Raman spectroscopy has proven most useful for the study of diagenetically
78 related minerals as tellurate and tellurite minerals often are. Some previous studies
79 using Raman spectroscopy have been undertaken by the authors to explore the
80 structure of minerals [11-20]. The aim of this paper is to present Raman of the
81 natural selected mixed anion mineral tlapallite which contains both tellurate and
82 tellurite anions and to discuss the spectra from a structural point of view. It is part of
83 systematic studies on the vibrational spectra of minerals of secondary origin in the
84 oxide supergene zone and their synthetic analogs.

85 86 **2. Experimental**

87 88 *2.1 Minerals*

89
90 The mineral tlapallite was sourced from Mina Bambollita, Moctezuma, Sonora,
91 Mexico. This is the type mineral. The composition of the same mineral, obtained
92 from different sources, has been reported by Anthony *et al.* (page 709) [21].

93 94 *2.2 Raman microprobe spectroscopy*

95
96 Crystals of the tlapallite mineral were placed and orientated on the stage of an
97 Olympus BHSM microscope which was equipped with 10x and 50x objectives as part
98 of a Renishaw 1000 Raman microscope system. The system also includes a
99 monochromator, filter system and Charge Coupled Device (CCD). Raman spectra

100 were excited by a HeNe laser (633 nm) at a resolution of 2 cm^{-1} in the range between
101 100 and 4000 cm^{-1} . Repeated acquisition using the highest magnification was
102 accumulated to improve the signal to noise ratio. Spectra were calibrated using the
103 520.5 cm^{-1} line of a silicon wafer.

104

105 Spectroscopic manipulation such as baseline adjustment, smoothing and
106 normalisation were performed using the Spectracalc software package GRAMS
107 (Galactic Industries Corporation, NH, USA). Band component analysis was
108 undertaken using the Jandel 'Peakfit' software package, which enabled the type of
109 fitting function to be selected and allows specific parameters to be fixed or varied
110 accordingly. Band fitting was done using a Gauss-Lorentz, cross-product function
111 with the minimum number of component bands used for the fitting process. The
112 Gauss-Lorentz ratio was maintained at values greater than 0.7 and fitting was
113 undertaken until reproducible results were obtained with squared correlations (r^2)
114 greater than 0.995.

115

116

117 **3. Results and discussion**

118

119 Farmer [22] states that very little research has been undertaken on the
120 vibrational spectroscopy of tellurates. As such very few papers have been
121 forthcoming. Only a few minerals with the tellurate anion have been discovered [2-
122 4]. The metatellurate anion TeO_4^{2-} should have T_d symmetry and therefore four
123 internal modes, namely A_1 (ν_1), E (ν_2) and $2F_2$ (ν_3 and ν_4). The orthotellurate ion,
124 TeO_6^{6-} will have octahedral symmetry but may be strongly distorted. Vibrational
125 modes for the tellurate anion should occur in the 620 to 650 cm^{-1} region and in the
126 290 to 360 cm^{-1} region. If the symmetry of the tellurate anion is reduced through for
127 example bonding to a cation as in the kuranakhite structure then the loss of
128 degeneracy will occur, and additional bands observed. Siebert [23] reported the
129 infrared spectra of selected synthetic tellurates and antimonates. The position of the
130 bands for the TeO_6^{6-} anion was defined by Siebert as ν_1 650 cm^{-1} (A_{1g}), ν_3 630 cm^{-1}
131 (E_g), ν_2 375 cm^{-1} (F_{2g}). For the compound H_6TeO_6 infrared bands were observed at
132 605 , 650 , 658 , 675 , 708 and 730 cm^{-1} and were assigned to TeO stretching vibrations.
133 In addition an intense band at 411 cm^{-1} is assigned to a δTeO bending mode

134 (presumably ν_4 vibration). For the compound $\text{Na}_2\text{H}_4\text{TeO}_6$ infrared bands were
135 observed at 429, 536, 587, 675 and 780 cm^{-1} . More complexity was observed in the
136 spectrum of $\text{K}_2\text{H}_4\text{TeO}_6 \cdot 3\text{H}_2\text{O}$. Siebert also provided data for the compound $(\text{H}_4\text{TeO}_4)_x$.
137 For this polytellurous acid, infrared bands were found at 450 cm^{-1} (δTeO) and
138 stretching modes at 600, 720, 800 cm^{-1} . According to Siebert the TeO_6^{6-} anion is
139 octahedral but is distorted. Thus infrared forbidden bands are activated.

140

141

142 The Raman spectrum of tlapallite in the 600 to 900 cm^{-1} region is shown in
143 Figure 1. The spectral profile displays Raman bands at 764 and 796 cm^{-1} , Raman
144 bands are observed also at 691 and 708 cm^{-1} . It is difficult to nominate a specific
145 cause for each of these bands but one possible suggestion is as follows: the higher
146 wavenumber bands may be attributed to the tellurate ion $(\text{TeO}_6)^{2-}$ and the lower
147 wavenumber bands to the tellurite anion $(\text{TeO}_3)^{2-}$. Thus, the Raman band at 796 cm^{-1}
148 is attributed to the $\nu_1(\text{TeO}_6)^{2-}$ symmetric stretching mode and the band at 764 cm^{-1} to
149 the $\nu_1(\text{TeO}_3)^{2-}$ symmetric stretching mode. The band at 708 cm^{-1} may be attributed to
150 the $\nu_3(\text{TeO}_6)^{2-}$ antisymmetric stretching mode and the band at 691 cm^{-1} to the ν_1
151 $(\text{TeO}_3)^{2-}$ antisymmetric stretching mode. The Raman spectrum in the 900 to 1700 cm^{-1}
152 region is shown in Figure 2. This spectral region is where the $(\text{SO}_4)^{2-}$ stretching
153 bands may be observed. The intense, sharp Raman band at 973 cm^{-1} is assigned to the
154 $\nu_1(\text{SO}_4)^{2-}$ symmetric stretching mode, whilst the two bands at 1062 and 1104 cm^{-1} are
155 assigned to the $\nu_3(\text{SO}_4)^{2-}$ antisymmetric stretching mode. The low intensity Raman
156 bands at 1474 and 1571 cm^{-1} may be associated with the protons via formation of OH
157 units. Alternatively, the bands may be associated with bands, associated with
158 amorphous carbon. Such bands may originate from handling of the sample and the
159 burning of organic residues by the incident laser.

160

161 A comparison may be made with the Raman spectra of other tellurate
162 minerals. In the Raman spectrum of xocomecatlite $\text{Cu}_3(\text{OH})_4\text{TeO}_4 \cdot \text{H}_2\text{O}$ a broad band
163 that may be decomposed into component bands at 710 , 763 and 796 cm^{-1} . These bands
164 are quite sharp. One possible assignment is the band at 796 cm^{-1} is ascribed to the
165 $\text{TeO}_4 \nu_1$ symmetric stretching mode and the two bands at 710 and 763 cm^{-1} to the
166 TeO_4 antisymmetric stretching mode. Two bands for of kuranakhite $\text{PbMn}^{4+}\text{Te}^{6+}\text{O}_6$
167 observed at 617 and 686 cm^{-1} are assigned to the $\text{Te}^{6+}\text{O}_6 \nu_1$ symmetric stretching

168 mode. The observation of two bands suggests the non equivalence of the Te^{6+}O_6 in the
169 structure. Such a concept would need to be confirmed by X-ray diffraction. The
170 broad band centred at 743 cm^{-1} is attributed to the Te^{6+}O_6 ν_3 antisymmetric stretching
171 mode. The width of this band may indicate that it is composed of a number of
172 overlapping bands. The assignment of the Te^{6+}O_6 stretching bands is at variance to
173 that proposed by Siebert. [23]

174

175

176 In terms of tellurite anion a comparison may be made with the Raman spectra
177 of other tellurite minerals. For example, two Raman bands for rajite observed at 754
178 and 731 cm^{-1} are assigned to the ν_1 $(\text{Te}_2\text{O}_5)^{2-}$ symmetric stretching mode. The two
179 bands at 652 and 603 cm^{-1} are assigned to the ν_3 $(\text{Te}_2\text{O}_5)^{2-}$ antisymmetric stretching
180 mode. An intense band observed at 734 cm^{-1} for denningite, is attributed to the ν_1
181 $(\text{Te}_2\text{O}_5)^{2-}$ symmetric stretching mode. The Raman band of denningite, at 674 cm^{-1} , is
182 assigned to the ν_3 $(\text{Te}_2\text{O}_5)^{2-}$ antisymmetric stretching mode. Two Raman bands for
183 zemannite are observed at 745 and 647 cm^{-1} . These bands are assigned to the ν_1
184 $(\text{TeO}_3)^{2-}$ symmetric stretching mode and the ν_3 $(\text{TeO}_3)^{2-}$ antisymmetric stretching
185 mode, respectively. Two Raman bands, observed at 763 and 791 cm^{-1} for emmonsite,
186 are assigned to the ν_1 $(\text{TeO}_3)^{2-}$ symmetric stretching mode whilst the Raman bands
187 displayed at 679 and 567 cm^{-1} are assigned to the ν_3 $(\text{TeO}_3)^{2-}$ antisymmetric stretching
188 mode.

189

190 The low wavenumber region of tlapallite, 100 to 600 cm^{-1} , is shown in Figure
191 3. This region displays those bands which are attributable to the $(\text{SO}_4)^{2-}$, $(\text{TeO}_3)^{2-}$ and
192 $(\text{TeO}_6)^{4-}$ bending modes. The complexity of the spectrum makes assignment difficult.
193 One possible set of assignments is as follows: the band at 610 cm^{-1} (Figure 1) may be
194 assigned to the $(\text{SO}_4)^{2-}$ ν_4 bending mode and the intense band at 438 cm^{-1} may be
195 attributed to the $(\text{SO}_4)^{2-}$ ν_2 bending mode. The two Raman bands of tlapallite, at 314
196 and 353 cm^{-1} , may be assigned to the $(\text{TeO}_3)^{2-}$ ν_2 (A_1) bending mode and the two
197 bands, at 383 and 419 cm^{-1} , may be assigned to the $(\text{TeO}_3)^{2-}$ ν_4 (E) bending mode.
198 The remaining bands, at 474 and 509 cm^{-1} , may be assigned to the $(\text{TeO}_6)^{4-}$ ν_4 and ν_2
199 bending modes. The Raman bands at 229 , 258 and 291 cm^{-1} may be associated with
200 MO and OMO stretching and bending vibrations where M may be Cu, Zn, Ca or Pb.

201

202 Raman bands for rajite, observed at (346, 370) and 438 cm⁻¹ are assigned to
203 the (Te₂O₅)²⁻ ν₂ (A₁) bending mode and ν₄ (E) bending mode. The very weak Raman
204 bands of denningite at 450 and 479 cm⁻¹ are assigned to the (Te₂O₅)²⁻ ν₄ (E) bending
205 modes and the bands at 349 and 381 cm⁻¹ are assigned to the (Te₂O₅)²⁻ ν₂ (A₁)
206 bending mode. Raman bands are observed at 372 and 408 cm⁻¹ for zemmanite and
207 397 and 414 cm⁻¹ for emmonsite, both of which may be due to the (TeO₃)²⁻ ν₂ (A₁)
208 bending mode. Two low intensity bands in the Raman spectrum of graemite, at 314
209 and 358 cm⁻¹, may be assigned to the (TeO₃)²⁻ ν₂ (A₁) bending mode. The intense
210 bands at 411, 438 and 471 cm⁻¹ may be assigned to the (TeO₃)²⁻ ν₄ (E) bending
211 mode. The sharp Raman band for teineite at 235 cm⁻¹ may be attributed to CuO
212 stretching vibrations. The two sharp bands for graemite at 257 and 291 cm⁻¹ may also
213 be attributed to CuO stretching vibrations.

214

215

216 The Raman spectrum of tlapallite in the 1800 to 3200 cm⁻¹ region is displayed
217 in Figure 4. The spectrum suffers from a low of signal to noise ratio. This is not
218 unexpected as there are no water or OH units in the tlapallite structure. The scale of
219 the spectrum has been increased. Bands in this spectral region may result from
220 induced OH units formed by the interaction of the protons with the sulphate, tellurite
221 or tellurate units. Bands are identified at around 1957, 2206, 2326, 2594, 2754, 2867
222 and 2926 cm⁻¹. These bands are attributed to OH stretching vibrations formed by the
223 interaction of the protons with the oxygen of the tellurate/tellurite units. Alternatively
224 some of these very low intensity bands may well be identifying surface contamination
225 by organic molecules, perhaps through handling. The bands in the 2850 to 2950 cm⁻¹
226 may well be assigned to CH stretching vibrations.

227

228 Studies have shown a strong correlation between OH stretching frequencies
229 and both O···O bond distances and H···O, hydrogen bond distances [24-27].

230 Libowitzky (1999) showed that a regression function can be employed relating the
231 hydroxyl stretching frequencies with regression coefficients better than 0.96 using
232 infrared spectroscopy [28]. The function is described as: ν₁ =

233 $(3592 - 304) \times 109^{\frac{-d(O-O)}{0.1321}}$ cm⁻¹. Thus, OH···O, hydrogen bond distances may be

234 calculated using the Libowitzky empirical function. The values for the OH stretching

235 vibrations listed above provide hydrogen bond distances of 2.537(0) Å (2206 cm⁻¹),
236 2.549(3) Å (2326 cm⁻¹), 2.580(7) Å (2594 cm⁻¹), 2.603(5) Å (2754 cm⁻¹), 2.622(7) Å
237 (2867 cm⁻¹) and 2.633(9) Å (2926 cm⁻¹) which are very short compared with that of
238 many secondary minerals. Normally, large hydrogen bond distances, which are
239 present in minerals such as perhamite, can also be seen in other mixed anion minerals,
240 such as peisleyite, where the distances range between 3.052(5) and 2.683(6) Å. Such
241 hydrogen bond distances are typical of secondary minerals. A range of hydrogen
242 bond distances are observed from reasonably strong to weak hydrogen bonding. This
243 range of hydrogen bonding contributes to the stability of the mineral. In the case of
244 tlapallite, the proton-tellurite interactions contribute to the stability of this tellurite
245 mineral to compensate for the lack of stability provided by the larger hydrogen bond
246 distances.

247

248

249 **4. Conclusions**

250

251 In nature, very few tellurate minerals exist. They may be subdivided according
252 to formula and structure. The tellurate ion is TeO₄²⁻ or TeO₆⁶⁻. Unlike sulfate,
253 tellurate is a good oxidizing agent; it can be reduced to tellurite or even tellurium
254 metal. As a result of this, the quantity of tellurite minerals greatly out numbers the
255 quantity of tellurate minerals. The ready reduction of the tellurate anion to the
256 tellurite anion leads to certain minerals such as tlapallite forming mixed anionic
257 species in which both the tellurate and tellurite ions exist.

258

259 The Raman spectrum of the mixed anion tellurate mineral tlapallite, has been
260 studied using Raman spectroscopy. Observed bands were tentatively assigned to the
261 stretching and bending vibrations of the tellurite anion, (TeO₃)²⁻, the tellurate anion
262 and sulphate anion. Because of the potential overlap of bands ascribed to the tellurate
263 and tellurite anions, assignment of bands is not simple. It is difficult to nominate a
264 specific cause for each of these bands but one possible suggestion is as follows: the
265 higher wavenumber bands may be assigned to the tellurate anion, (TeO₆)²⁻, and the
266 lower wavenumber bands to the tellurite anion, (TeO₃)²⁻. Thus, the Raman band at
267 796 cm⁻¹ may be assigned to the ν₁ (TeO₆)²⁻ symmetric stretching mode and the band
268 at 764 cm⁻¹ to the ν₁ (TeO₃)²⁻ symmetric stretching mode. The band at 708 cm⁻¹ may

269 be assigned to the ν_3 $(\text{TeO}_6)^{2-}$ antisymmetric stretching mode and the band at 691 cm^{-1}
270 to the ν_1 $(\text{TeO}_3)^{2-}$ antisymmetric stretching mode. The band at 610 cm^{-1} may be
271 assigned to the $(\text{SO}_4)^{2-}$ ν_4 bending mode. The intense band at 438 cm^{-1} may be
272 attributed to the to the $(\text{SO}_4)^{2-}$ ν_2 bending mode. The two Raman bands of tlapallite at
273 314 and 353 cm^{-1} may be assigned to the $(\text{TeO}_3)^{2-}$ ν_2 (A_1) bending mode and the two
274 bands for teineite at 383 and 419 cm^{-1} may be assigned to the $(\text{TeO}_3)^{2-}$ ν_4 (E) bending
275 mode. The remaining bands at 474 and 509 cm^{-1} may be assigned to the $(\text{TeO}_6)^{4-}$ ν_4
276 and ν_2 bending modes.

277

278 **Acknowledgements**

279

280 The financial and infra-structure support of the Queensland University of
281 Technology Inorganic Materials Research Program of the School of Physical and
282 Chemical Sciences is gratefully acknowledged. The Australian Research Council
283 (ARC) is thanked for funding the instrumentation.

284

285

286

287 **REFERENCES**

288

- 289 [1] J.D. Dana, Dana's Manual of Mineralogy, by W. E. Ford. 22nd edition, Wiley
290 London 2006
- 291 [2] A.C. Roberts, J.D. Grice, L.A. Groat, A.J. Criddle, R.A. Gault, R.C. Erd, E.A.
292 Moffatt, *Can. Min.* 34 (1996) 49-54.
- 293 [3] A.C. Roberts, T.S. Ercit, A.J. Criddle, G.C. Jones, R.S. Williams, F.F.
294 Cureton, II, M.C. Jensen, *Min. Mag.* 58 (1994) 417-424.
- 295 [4] S.A. Williams, *Min. Mag.* 40 (1975) 221-226.
- 296 [5] S.A. Williams, M. Duggan, *Min. Mag.* 42 (1978) 183-186.
- 297 [6] R.L. Frost, J. Cejka, G.A. Ayoko, M.J. Dickfos, *J. Raman Spectrosc.* 39
298 (2008) 374-379.
- 299 [7] R.L. Frost, M.J. Dickfos, J. Cejka, *J. Raman Spectrosc.* 39 (2008) 582-586.
- 300 [8] R.L. Frost, M.C. Hales, D.L. Wain, *J. Raman Spectrosc.* 39 (2008) 108-114.
- 301 [9] R.L. Frost, E.C. Keeffe, *J. Raman Spectrosc.* in press (2008).
- 302 [10] S.J. Palmer, R.L. Frost, G. Ayoko, T. Nguyen, *J. Raman Spectrosc.* 39 (2008)
303 395-401.
- 304 [11] R.L. Frost, J.M. Bouzaid, *J. Raman Spectrosc.* 38 (2007) 873-879.
- 305 [12] R.L. Frost, J.M. Bouzaid, W.N. Martens, B.J. Reddy, *J. Raman Spectrosc.* 38
306 (2007) 135-141.
- 307 [13] R.L. Frost, J. Cejka, *J. Raman Spectrosc.* 38 (2007) 1488-1493.
- 308 [14] R.L. Frost, J. Cejka, G.A. Ayoko, M.L. Weier, *J. Raman Spectrosc.* 38 (2007)
309 1311-1319.
- 310 [15] R.L. Frost, J. Cejka, M.L. Weier, *J. Raman Spectrosc.* 38 (2007) 460-466.
- 311 [16] R.L. Frost, J. Cejka, M.L. Weier, W.N. Martens, G.A. Ayoko, *J. Raman*
312 *Spectrosc.* 38 (2007) 398-409.
- 313 [17] R.L. Frost, M.J. Dickfos, *J. Raman Spectrosc.* 38 (2007) 1516-1522.
- 314 [18] R.L. Frost, S.J. Palmer, J.M. Bouzaid, B.J. Reddy, *J. Raman Spectrosc.* 38
315 (2007) 68-77.
- 316 [19] R.L. Frost, C. Pinto, *J. Raman Spectrosc.* 38 (2007) 841-845.
- 317 [20] R.L. Frost, M.L. Weier, P.A. Williams, P. Leverett, J.T. Kloprogge, *J. Raman*
318 *Spectrosc.* 38 (2007) 574-583.
- 319 [21] J.W. Anthony, R.A. Bideaux, K.W. Bladh, M.C. Nichols, *Handbook of*
320 *Mineralogy*, Mineral Data Publishing, Tuscon, Arizona, USA, 2000.
- 321 [22] V.C. Farmer, Editor, *Mineralogical Society Monograph 4: The Infrared*
322 *Spectra of Minerals*, 1974.
- 323 [23] H. Siebert, *Z. anorg. u. allgem. Chem.* 301 (1959) 161-170.
- 324 [24] J. Emsley, *Chem. Soc. Rev.* 9 (1980) 91-124.
- 325 [25] H. Lutz, *Struct. Bond.* 82 (1995) 85-103.
- 326 [26] W. Mikenda, *J. Mol. Struct.* 147 (1986) 1-15.
- 327 [27] A. Novak, *Struct. Bond.* 18 (1974) 177-216.
- 328 [28] E. Libowitzky, *Monats. Chem.* 130 (1999) 1047-1049.

329

330

331

List of Figures

332

333

334 **Figure 1 Raman spectrum of tlappalite in the 600 to 900 cm⁻¹ region**

335

336 **Figure 2 Raman spectrum of tlappalite in the 900 to 1700 cm⁻¹ region**

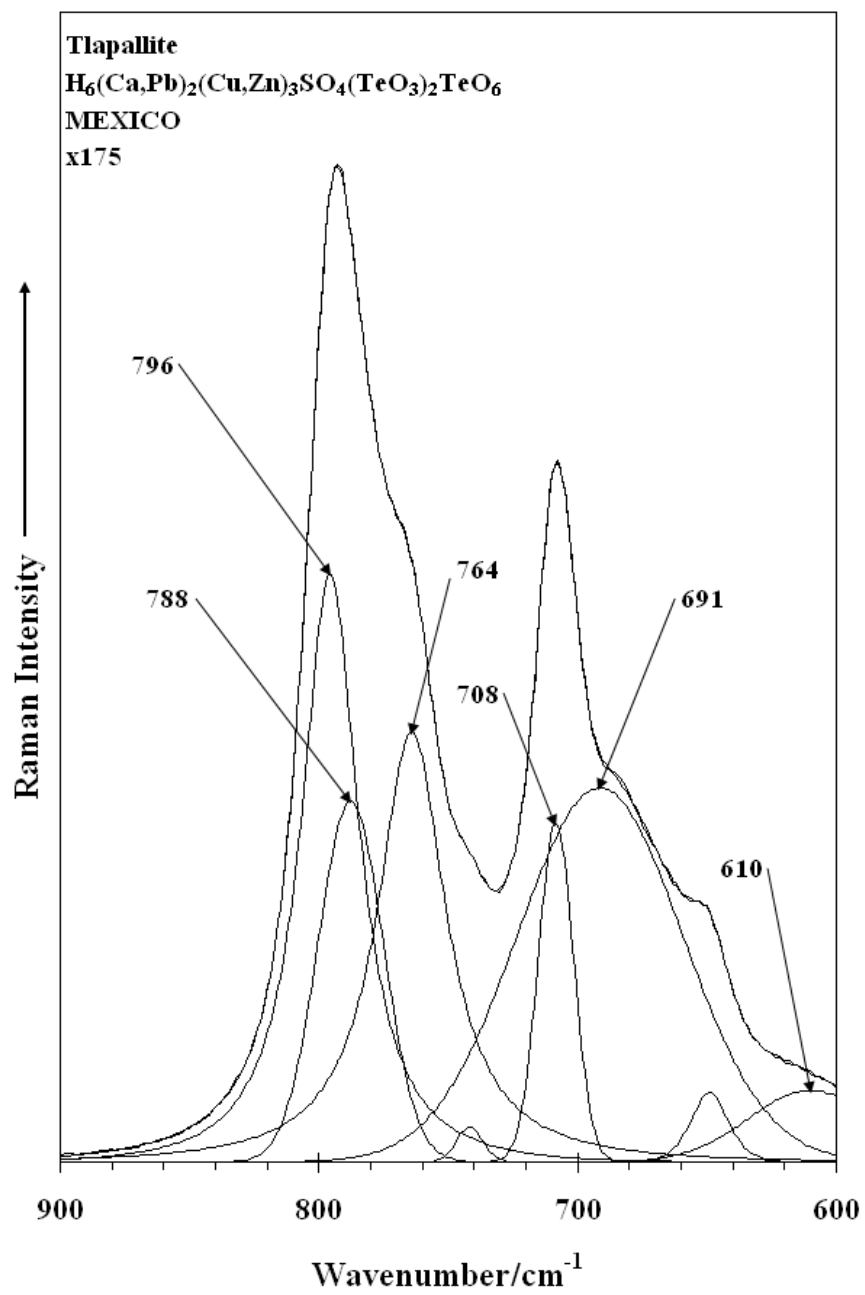
337

338 **Figure 3 Raman spectrum of tlappalite in the 100 to 600 cm⁻¹ region**

339

340 **Figure 4 Raman spectrum of tlappalite in the 1800 to 3200 cm⁻¹ region**

341



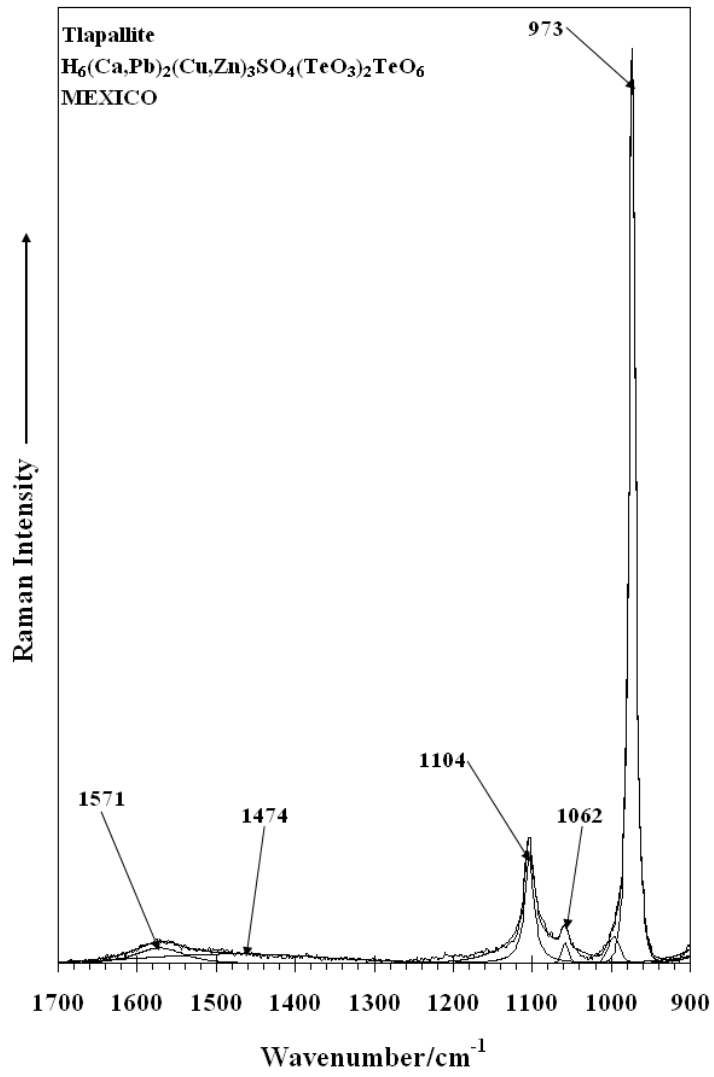
342

343

344 **Figure 1 tlapallite**

345

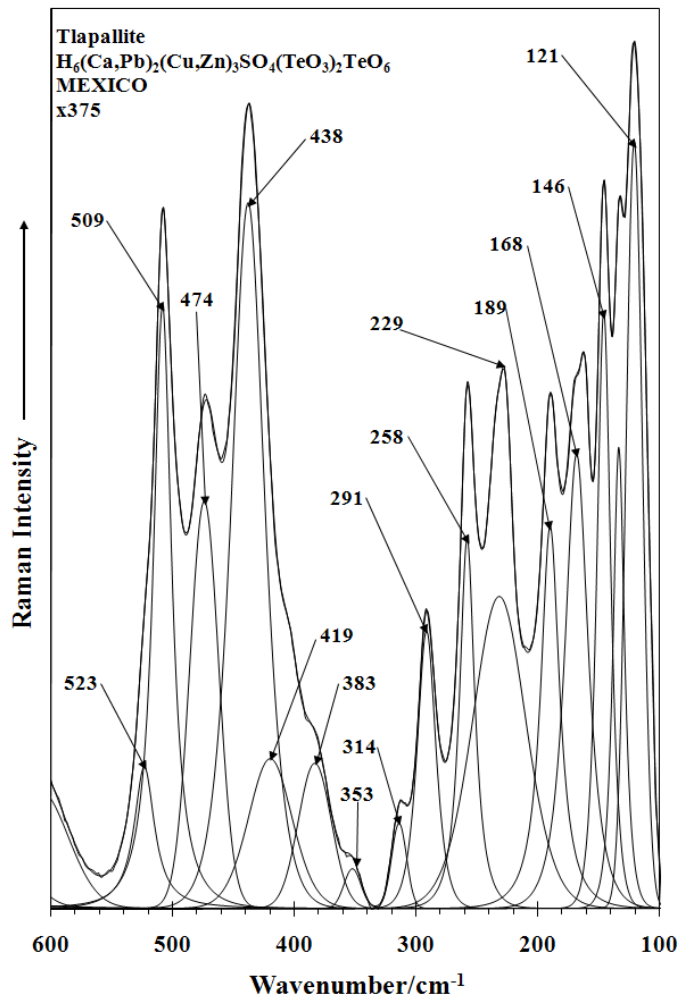
346



347

348

349 **Figure 2**

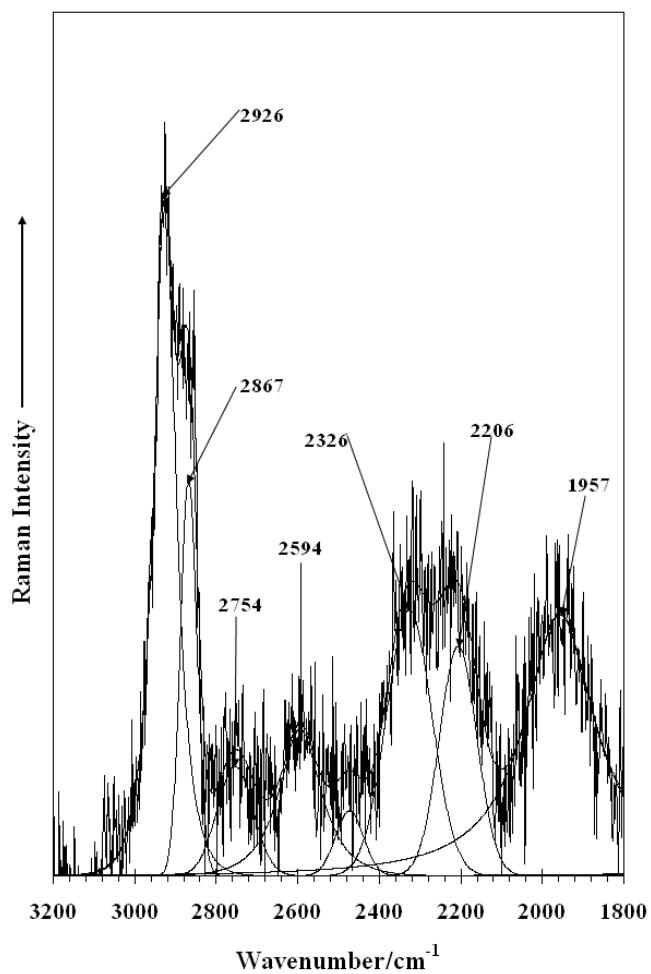


351

352

353 **Figure 3 tlapallite**

354



355

356

357 **Figure 4**

358

359